

Observational characteristics of dense cores with deeply embedded young protostars

D. STAMATELLOS, A.P. WHITWORTH and S.P. GOODWIN

School of Physics & Astronomy, Cardiff University, 5 The Parade, CF24 3YB, Cardiff, UK

Received <date>; accepted <date>; published online <date>

Abstract. Class 0 objects, which are thought to be the youngest protostars, are identified in terms of NIR or radio emission and/or the presence of molecular outflows. We present combined hydrodynamic and radiative transfer simulations of the collapse of a star-forming molecular core, which suggest two criteria for identifying dense cores with deeply embedded very young protostars that may not be observable in the NIR or radio with current telescopes. We find that cores with protostars are relatively warm ($T > 15$ K) with their SEDs peaking at wavelengths $< 170\mu\text{m}$, and they tend to appear circular.

Key words: stars: formation – ISM: clouds – dust, extinction – methods: numerical – radiative transfer – hydrodynamics

©0000 WILEY-VCH Verlag GmbH & Co. KGaA, Weinheim

1. Introduction

Class 0 objects, the youngest protostars identified so far, are distinguished from prestellar cores, their precursors, based on 2 criteria (see André et al. 2000), (i) the presence of a NIR source in the centre of the core, or (ii) the presence of compact radio emission or molecular outflows. These criteria depend on the sensitivity of the telescope used. Very young protostars are difficult to observe in the NIR, because they are deeply embedded. Additionally, the amount of their radio emission is uncertain (see Gibb 1999), and probably very low (Neufeld & Hollenbach 1996). Thus, a null detection with a specific telescope does not necessarily mean that a source does not exist. This was demonstrated recently with the core L1014 which was thought to be prestellar because no source was detected by IRAS, but later was suggested to be protostellar after a NIR source was detected by the more sensitive SPITZER (Young et al. 2004). Hence it is important to consider ways in which the presence of young embedded protostars might be inferred indirectly. In this paper we present SPH simulations of the collapse of a turbulent molecular core, combined with 3-dimensional Monte Carlo radiative transfer simulations at different stages of this collapse. The simulations predict dust temperature fields, SEDs, and isophotal maps of very young protostars that are deeply embedded in their parental cores, and provide criteria for distinguishing between genuine prestellar cores and cores that contain very young protostars (Stamatellos et al. 2005).

2. The model

We use the SPH code DRAGON (Goodwin et al. 2004) to simulate the dynamics of a collapsing molecular core and the Monte Carlo radiative transfer code PHAETHON (Stamatellos & Whitworth 2003, 2005; Stamatellos et al. 2004) to treat the radiative transfer within the core, at different time-frames during its collapse.

2.1. The collapse of a molecular cloud

The initial conditions in the core, before the collapse, are set according to observations (e.g. Kirk et al. 2005). Prestellar cores have typical extents from 2000 to > 15000 AU, and masses from 0.05 to $10 M_{\odot}$. Their density profiles are flat in their centre and fall off as r^{-n} , where $n = 2 - 4$. These features are well represented by a Plummer-like density profile (Plummer 1915),

$$\rho = \frac{\rho_0}{(1 + (r/r_0)^2)^2}, \quad r < r_B. \quad (1)$$

The density profile is almost flat for $r < r_0$, and falls off as r^{-4} in the outer envelope ($r > r_0$). We set $\rho_0 = 3 \times 10^{-18} \text{ g cm}^{-3}$, $r_0 = 5,000$ AU, and $r_B = 50,000$ AU. The core mass is then $5.4 M_{\odot}$. We impose a low level of turbulence ($\alpha_{\text{TURB}} \equiv E_{\text{TURB}}/|E_{\text{GRAV}}| = 0.05$).

The collapse of the turbulent core leads to the formation of a single star surrounded by a disc, and the material in the disc then slowly accretes onto the star. A sink particle, representing the star and the inner part of the disc, is created

Table 1. Model parameters

id	time (yr)	$M_*(M_\odot)$	R_S (AU)	Z_S (AU)	$M_S(M_\odot)$	$\dot{M}_*(M_\odot/\text{yr})$	$L_{\text{TOT}}(L_\odot)$	T_* (K)	description
t1	5.3×10^4	-	-	-	-	-	-	-	prestellar core
t3	6.0×10^4	0.20	4.0	0.4	0.09	1×10^{-5}	27.2	7650	Class 0 protostar
t5	6.9×10^4	0.53	4.0	0.4	0.01	4×10^{-7}	2.5	4200	protostar is off centre

Z_S, R_S : Smartie dimensions

M_* : Stellar mass

T_* : Star temperature

M_S : Smartie mass

\dot{M}_* : Accretion rate onto the central star

L_{TOT} : Total star luminosity (intrinsic +accretion)

where the density first exceeds $\rho_{\text{CRIT}} = 10^{-11} \text{ g cm}^{-3}$. We use a newly developed type of sink called a *smartie*, which is a rotating oblate spheroid. The star is a point mass at the centre of the smartie. The smartie gains mass from the accreting material and can lose mass by ejecting material in the form of protostellar jets. The jets are simulated by SPH particles which are created at rate $0.1TM_S/t_{\text{VISC}}$ and launched along the rotation axis with speed 100 km s^{-1} to form a bipolar outflow. These jets push the surrounding material aside and create hourglass cavities about the smartie rotation axis (see Stamatellos et al. 2005 for details).

2.2. Radiative transfer

We perform radiative transfer simulations on 3 time-frames during the collapse of a star-forming core (see Table 1). We focus our attention just before and just after the formation of the first protostar in the core.

For the radiative transfer simulations, we use a version of PHAETHON, a Monte Carlo radiative transfer code which we have developed and optimised for radiative transfer simulations on SPH density fields. The main new features of the optimised version are (i) that it uses the tree structure inherent within the SPH code to construct a grid of cubic radiative transfer (RT) cells, spanning the entire computational domain, the *global grid*; and (ii) that in addition it constructs a local grid of RT cells around each star, a *star grid*, representing a flared disc, to capture the steep temperature gradients that are expected in the vicinity of a star (Stamatellos & Whitworth 2005).

The core is illuminated externally by the interstellar radiation field and internally by the newly formed protostar (once it has formed). For the external radiation field we adopt a revised version of the Black (1994) interstellar radiation field, which consists of radiation from giant stars and dwarfs, thermal emission from dust grains, cosmic background radiation, and mid-infrared emission from transiently heated small PAH grains (André et al. 2003). The protostar luminosity is dominated by the luminosity due to accretion since the mass of the young protostar is small ($< 0.6 M_\odot$) and the accretion rate is high ($> 10^{-7} M_\odot/\text{yr}$).

3. Characteristics of prestellar cores and young protostars

3.1. Dust temperatures

In Fig. 1 we present the density fields and dust-temperature fields for the 3 time-frames in Table 1. We plot the density

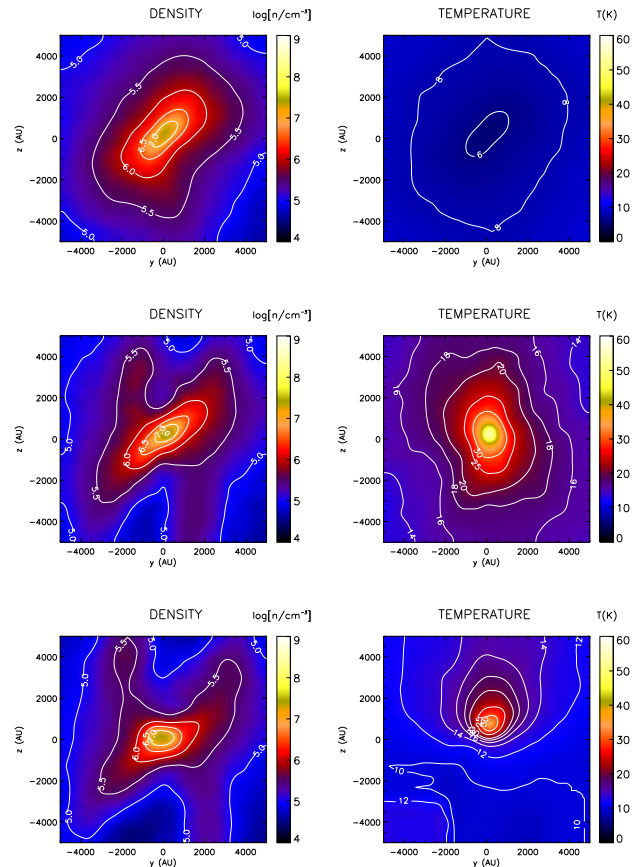


Fig. 1. Cross sections of density and dust temperature on a plane parallel to the $x = 0$ plane of 3 different time-frames (first row: *collapsing prestellar core*; second row: *Class 0 object*; third row: *Class 0 object*).

and the temperature on a cross section through the computational domain parallel to the $x = 0$. This plane passes through the protostar, or, if there is no protostar (as in the first time-frame), through the densest part of the core. The plots show only the central region of the core ($5000 \text{ AU} \times 5000 \text{ AU}$).

Our results for the temperature are broadly similar to those of previous 1D and 2D studies of prestellar cores and Class 0 objects (Evans et al. 2001; Zucconi et al. 2001; Shirley et al. 2002; Stamatellos & Whitworth 2003). The prestellar core is quite cold (5 to 20 K). As soon as a protostar forms, the region around it becomes very hot (up to the dust destruction temperature), but the temperature drops below $\sim 20 \text{ K}$ beyond a few 1000 AU from the protostar, be-

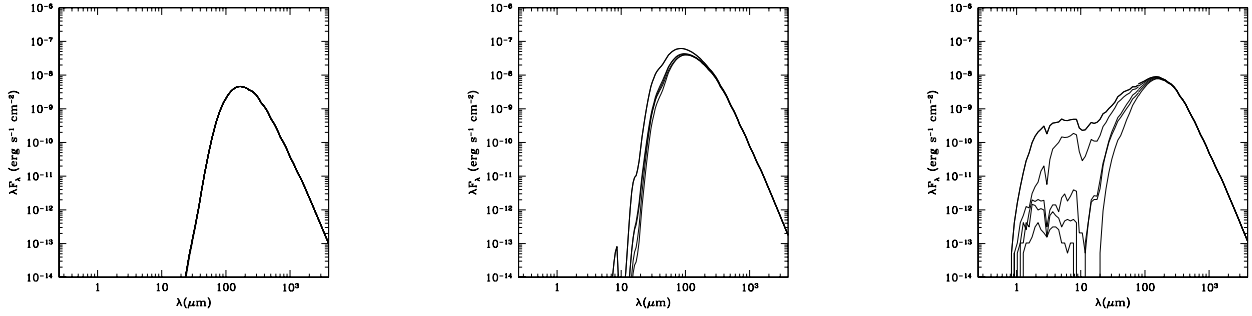


Fig. 2. SEDs of 3 different time-frames from 6 different angles (the SED is weakly dependent on viewing angle so that some of the curves overlap; the flux is higher when the protostar is viewed pole-on, i.e. through the hourglass cavity that is created by the jets). **(a)** first column - *collapsing prestellar core*. The SED peaks at $\sim 190 \mu\text{m}$ (temperature $T_{\text{EFF}} \sim 13 \text{ K}$). **(b)** second column - *Class 0 object*. The emission of the system peaks at $\lambda \sim 80$ to $100 \mu\text{m}$ (depending on the observer's viewing angle) ($T_{\text{EFF}} \sim 25$ to 31 K). **(c)** third column - *Class 0 object*. The protostar has moved out of the central region by $\sim 100 \text{ AU}$, and the attenuated stellar emission can be seen at short wavelengths (1 to $50 \mu\text{m}$). The peak of the cloud emission is at $\lambda \sim 150 \mu\text{m}$ ($T_{\text{EFF}} \sim 17 \text{ K}$).

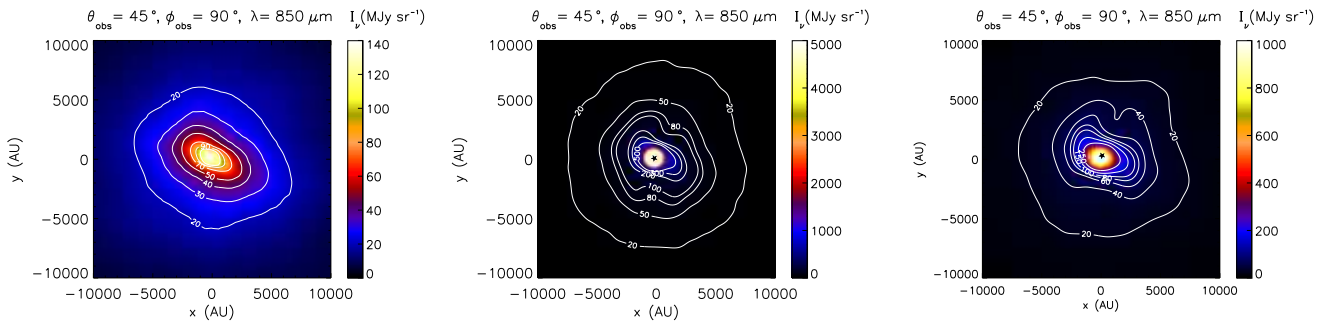


Fig. 3. $850 \mu\text{m}$ isophotal maps of 3 different time-frames (first column: *collapsing prestellar core*; second column: *Class 0 object*; third column: *Class 0 object*). Cores with protostars (second and third columns) are more centrally condensed than prestellar cores (first column). The axes (x, y) refer to the plane of sky as seen by the observer

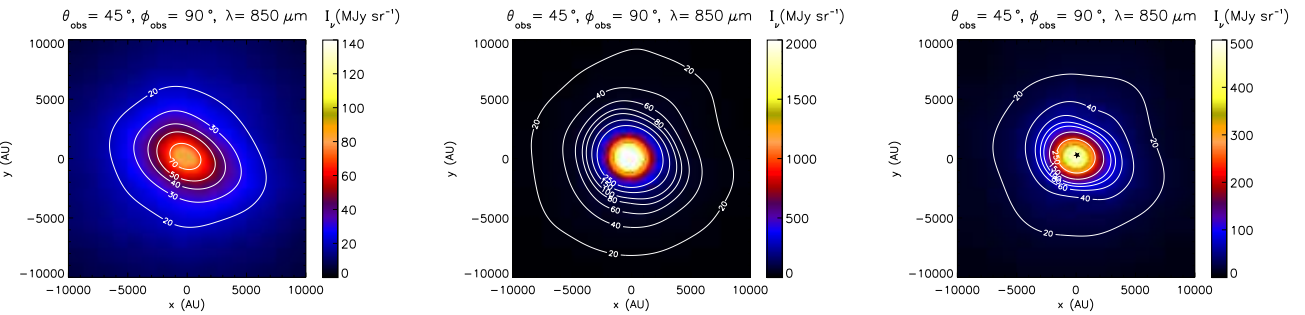


Fig. 4. As in Fig. 3, but after convolving with a Gaussian beam (FWHM = 2300 AU , e.g. $15''$ for a core at 150 pc). Cores with protostars appear more circular, but otherwise similar to the prestellar core.

cause of the high optical depth in the dense accretion flow onto the protostar.

3.2. SEDs

The SEDs of the 3 time-frames in Table 1 are presented in Fig. 2. These SEDs have been calculated assuming that the core is at 140 pc . SEDs are plotted for 6 different viewing angles, i.e. 3 polar angles ($\theta = 0^\circ, 45^\circ, 90^\circ$) and 2 azimuthal angles ($\phi = 0^\circ, 90^\circ$).

The effective temperature of the core, as inferred from the peak of the SED, rises and falls with the accretion luminosity of the protostar. For a prestellar core, the SED peaks at $\sim 190 \mu\text{m}$, implying $T_{\text{EFF}} \sim 13 \text{ K}$. Once the protostar has formed and inputs energy into the system, the peak moves steadily to shorter wavelengths, reaching $\sim 80 \mu\text{m}$ ($T_{\text{EFF}} \sim 31 \text{ K}$) as the accretion luminosity reaches its maximum, and then moving back to longer wavelengths again as the accretion luminosity declines. By the final frame it has reached $\sim 150 \mu\text{m}$ ($T_{\text{EFF}} \sim 17 \text{ K}$).

The peak of the SED of a prestellar core is independent of viewing angle, since the core is optically thin to the radiation it emits. In contrast, the peak of the SED of a Class 0 object does depend on viewing angle, albeit weakly, because of the presence of an optically thick disc around the protostar. However, even allowing for variations in the viewing angle, the SED of a Class 0 object does not peak at the wavelengths characteristic of prestellar cores ($\sim 190 \mu\text{m}$).

Our model predicts that a young protostar embedded in a core is not observable in the NIR, *unless* it is displaced from the central high-density region. This refers to the very early stages of protostar formation. This result contradicts the recent results of Whitney et al. (2003) and Young et al. (2004); they predict that NIR radiation from a deeply embedded young protostar is observable. We attribute the differences to the fact that these models use different densities for the region near the protostar and different opacities. Ultimately, the density distribution within 500 AU of the centre of a core or a protostar is not well constrained, and therefore radiative transfer calculations have to rely on theoretical models of core collapse. Dust opacities are also poorly constrained (e.g. Bianchi et al. 2003).

4. Isophotal maps

In Fig. 3 we present isophotal maps at $850 \mu\text{m}$ for the 3 time-frames in Table 1. At $850 \mu\text{m}$ the core is optically thin, and the temperature does not vary much (~ 10 to 20 K, apart from the region very close to the protostar in time-frames τ_3 and τ_5), so the maps are effectively column density maps. Class 0 objects are more centrally condensed than prestellar cores. They also show more structure, due to bipolar outflows, which clear low-density cavities.

In Fig. 4 we present the isophotal maps after convolving them with a Gaussian beam having $\text{FWHM} = 2,300$ AU. Assuming the cloud is 150 pc away, this corresponds to an angular resolution of $15''$, which is similar to the beam size of current submm and mm telescopes (e.g. SCUBA, IRAM). On these maps, Class 0 objects look very similar to prestellar cores, apart from the fact that they tend to appear more circular and featureless.

The reason for this is that the emission from a core that contains a protostar is concentrated in the central few hundred AU, and so, when it is convolved with a $2,300$ AU beam, it produces an image rather like the beam, i.e. round and smooth. In contrast, the emission from a prestellar cores has structure on scales of several thousand AU, much of which survives convolution with a $2,300$ AU beam. Thus we should expect cores that contain protostars to appear rounder than prestellar cores, and indeed this is what is observed (Goodwin et al. 2002).

5. Conclusions

Our simulations indicate that a newly-formed protostar may not be observable in the NIR with current telescopes, because

it is too deeply embedded. This result reflects the high densities which our model predicts in the immediate surroundings of a newly-formed protostar. Thus, it is suggested that cores with *no observed* NIR radiation may in fact contain the *youngest* protostars.

Based on the results of the combined hydrodynamic and radiative transfer simulations, we propose two criteria for identifying cores which – despite appearing to be prestellar – may harbour very young protostars:

(a) They are warm ($T > 15$ K) as indicated by the peak of the SED of the core ($\lambda_{\text{peak}} < 170 \mu\text{m}$). This criterion requires that the peak of the SED can be measured to an accuracy of $\sim 30 \mu\text{m}$, which should be feasible with observations in the far-IR from ISO and the upcoming Herschel mission, and in the mm/submm region from SCUBA and IRAM. We have presumed that the core is heated by the average interstellar radiation field, and the criterion would have to be modified for a core irradiated by a stronger or weaker radiation field.

(b) Their submm/mm isophotal maps are circular, at least in the central 2000 to 4000 AU.

These criteria can be used to identify “warm”, circular cores that may potentially contain the youngest protostars. These cores can then be probed by deep radio observations with the VLA. Recently, we carried out 3.6 cm VLA observations for 4 of these cores and results will be presented in a future publication.

Acknowledgements. We thank P. André for providing the revised version of the Black (1994) ISRF, that accounts for the PAH emission. We also thank D. Ward-Thompson for useful discussions and suggestions. This work was partly supported from the EC Research Training Network “The Formation and Evolution of Young Stellar Clusters” (HPRN-CT-2000-00155), and partly by PPARC grant PPA/G/O/2002/00497.

References

- André, P., Ward-Thompson, D., & Barsony, M. 2000, *Protostars and Planets IV*, 59
- André, P., Bouwman, J., Belloche, A., & Hennebelle, P. 2003, *SFCHEM 2002: Chemistry as a Diagnostic of Star Formation*, proceedings of a conference held August 21-23, 2002 at University of Waterloo, Waterloo, Ontario, Canada N2L 3G1. Edited by Charles L. Curry and Michel Fich. NRC Press, Ottawa, Canada, 2003, p. 127., 127
- Bianchi, S., Gonçalves, J., Albrecht, M., Caselli, P., Chini, R., Galli, D., & Walmsley, M. 2003, *A&A*, 399, L43
- Black, J. H. 1994, *ASP Conf. Ser. 58: The First Symposium on the Infrared Cirrus and Diffuse Interstellar Clouds*, 355
- Evans, N. J., Rawlings, J. M. C., Shirley, Y. L., & Mundy, L. G. 2001, *ApJ*, 557, 193
- Gibb, A. G. 1999, *MNRAS*, 304, 1
- Goodwin, S. P., Ward-Thompson, D., & Whitworth, A. P., 2002, *MNRAS*, 330, 769
- Goodwin, S. P., Whitworth, A. P., & Ward-Thompson, D. 2004, *A&A*, 414, 633
- Kirk, J. M., Ward-Thompson, D., & André, P. 2005, *MNRAS*, 360, 1506
- Neufeld, D. A. & Hollenbach, D. J. 1996, *ApJ*, 471, L45
- Plummer, H. C., 1915, *MNRAS*, 76, 107
- Shirley, Y. L., Evans, N. J., & Rawlings, J. M. C. 2002, *ApJ*, 575, 337

- Stamatellos, D. & Whitworth, A. P. 2003, *A&A*, 407, 941
Stamatellos, D., & Whitworth, A. P. 2005, *A&A*, 439, 153
Stamatellos, D., Whitworth, A. P., André, P., & Ward-Thompson, D.
2004, *A&A*, 420, 1009
Stamatellos, D., Whitworth, A. P., Boyd, D. F. A., & Goodwin, S. P.
2005, *A&A*, 439, 159
Whitney, B. A., Wood, K., Bjorkman, J. E., & Wolff, M. J. 2003,
ApJ, 591, 1049
Young, C. H., et al. 2004, *ApJS*, 154, 396
Zucconi, A., Walmsley, C. M., & Galli, D. 2001, *A&A*, 376, 650